Active Balancing of a Flexible Rotor in Active Magnetic Bearings

Francis Fomi Wamba
Mechatronik im Maschinenbau, Technische Universität Darmstadt
64287 Darmstadt, Germany
fomi@mim.tu-darmstadt.de

Rainer Nordmann
Mechatronik im Maschinenbau, Technische Universität Darmstadt
64287 Darmstadt, Germany
nordmann@mim.tu-darmstadt.de

ABSTRACT

Vibrations mostly caused by mass-unbalance reduce the reliability, the operational safety and the life cycle of high speed rotors. This leads to costly outages and unscheduled maintenances. Commonly used offline balancing processes are very expensive for the machine user. To reduce these costs and to realize an uninterrupted control of the balancing states during operation, a complete automatic balancing strategy is proposed. It is based on the combination of the active magnetic bearings, the active balancing devices, and the drive motor and is applied to a flexible low pressure shaft of a helicopter engine test rig. Experimental results validate the efficiency of the proposed strategy.

Keywords: flexible rotor, active balancing devices, active magnetic bearings, influence coefficients method.

INTRODUCTION

Today´s rotating machinery (machine tools, turbo machinery and aircraft gas turbine engine) have to be more efficient, have to operate at higher speeds and hence have to pass as many as possible critical speeds. The vibrations during operation are mainly related to rotor mass unbalance, typically caused by manufacturing tolerances, assembling imprecision, or material accumulation and so on. Consequently the precision, the reliability, the operational safety, and the life cycle of high speed machinery decreases. By excessive vibration levels critical speeds can not be passed and the operation speed can not be reached. Therefore unplanned, forced outages are necessary to perform maintenance. Furthermore, commonly used offline balancing processes are very expensive for the machine user due to several rundowns to add test weights, increased manpower as well as great expenditure of time.

The application of active magnetic bearings (AMBs) in combination with active balancing devices (ABDs) allow for a partially automation of the balancing process and combines the advantages of both systems [4]. The great benefits of AMBs particularly in the field of high speed rotating machinery are: contactless support of the rotor, control of rotor motions (unbalance compensation or auto balancing), active override of the rotor during operation, identification, monitoring, and the use as measuring tool. However AMBs dissipate lots of energy and can not compensate the unbalance forces at higher rotating speeds due to saturated actuation. These restrictions of the AMBs can be avoided by usage of the ABDs. The ABDs allow for contactless generated test and compensation weights during operation i.e. they allow to control the unbalance state of the rotating machinery by means of a stepper drive motor principle. In this contribution the optimal efficiency of the ABDs is realized with the influence coefficients method.

For complete automation of the balancing process and further optimization, the drive motor (DM) has to be combined with the both above mentioned active systems (AMBs, ABDs) as shown in Fig. 1.

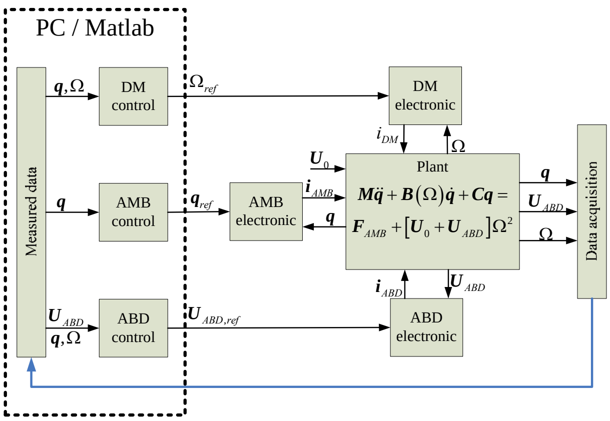

Fig. 1: Principle of the automatic balancing strategy

The new benefits of the developed automatic balancing strategy are the reduction of the man power and the automatic control of vibrations so that a user defined vibration threshold up to the operating speed is not violated. This vibration threshold is selected as criteria to enable or disable the automatic balancing program. If the vibration level exceeds the threshold, the automatic balancing program is activated and forces the DM to stop the run up at the actual speed. After reducing the vibration below the threshold via the ABDs, the automatic balancing program deactivates itself and enables the DM to continue its run up to the operating speed. In that way vibration levels can be limited, critical rotor speeds can be passed and the precision, the reliability, and the operational safety of high speed machinery are assured. A method to determine automatically the vibration limit depending on the measurement accuracy and resiudal unbalance as well as to generate appropriate test weights to avoid numerical errors by the unbalance calculation will be presented.

In section II of this paper the test rig is presented, followed by a short description of the active components and the investigation of the shaft's dynamic behavior. The theory for an automatic balancing strategy is described in section III, followed by an experimental validation in section IV. Finally a conclusion is given in section V.

TESTRIG

Fig. 2 shows the test rig to investigate the automatic unbalance compensation.

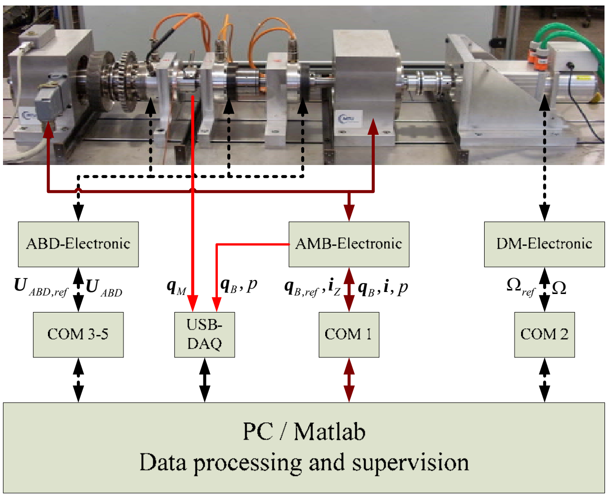

Fig. 2: Testrig

The configuration consists of three active systems: active magnetic bearings (AMBs), active balancing devices (ABDs) and drive motor (DM). Each of them corresponds to a typical mechatronic system with typical mechatronic components. They can communicate via a serial interface with a personal computer (PC). In the center of the rotor, the signals of two additional position sensors are fed to the PC via an USB data acquisition device. The PC gets measured data (rotating speed Ω, shaft oscillations $\boldsymbol{q}$ and generated unbalances $\boldsymbol{U}_{ABD}$) and sets the reference values (Ω_{ref} and $\boldsymbol{U}_{ABD,ref}$) for the active systems.

Flexible shaft in active magnetic bearings

The main component of the test rig is a low pressure shaft of a helicopter engine radially supported by active magnetic bearings (Fig. 3).

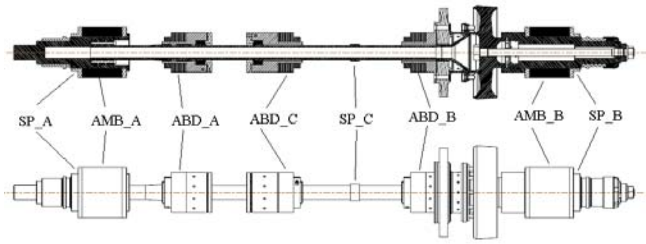

Fig. 3: shaft with actuator and sensor planes

The hollow shaft has a diameter of 25 mm, a wall thickness of 3.5 mm and includes two turbines stages with removed blades. With a length of 1100 mm the overall weight of the shaft is approx. 25.4 kg. The shaft can be split in to two parts to allow for the assembly of the three ABDs. It is connected to the drive motor with a torsionally stiff clutch. This clutch decouples the shaft in axial and radial directions so that disturbances from the motor drive do not affect the AMB-rotor system.

For a successful overcritical operation of the shaft in the AMBs and for a suitable placement of the balancing devices and sensor planes on the shaft, the knowledge about the dynamic behavior of the whole system is essential. With the assumption of linear system behavior the shaft dynamic can be described completely by the following differential equation.

$$\boldsymbol{M}\ddot{\boldsymbol{q}} + [\boldsymbol{D} + \Omega\boldsymbol{G}]\dot{\boldsymbol{q}} + \boldsymbol{C}\boldsymbol{q} = \boldsymbol{F} \qquad \text{(eq.1)}$$

The vector $\boldsymbol{q}$ denotes the generalized coordinate to describe the motion, Ω the rotating speed, $\boldsymbol{F}$ the vector of input forces, $\boldsymbol{M}$ the mass matrix, $\boldsymbol{D}$ damping matrix, $\boldsymbol{G}$ the gyroscopic matrix, and $\boldsymbol{C}$ the stiffness matrix of the free-free rotor. The modal parameters are calculated by the use of the finite element method. The shaft dynamics is analyzed up to the maximum rotating speed of the motor drive (500 Hz). The results of the FE-calculation of the shaft (mode shapes and eigenfrequencies) without bearings in free-free conditions are shown in Fig. 4.

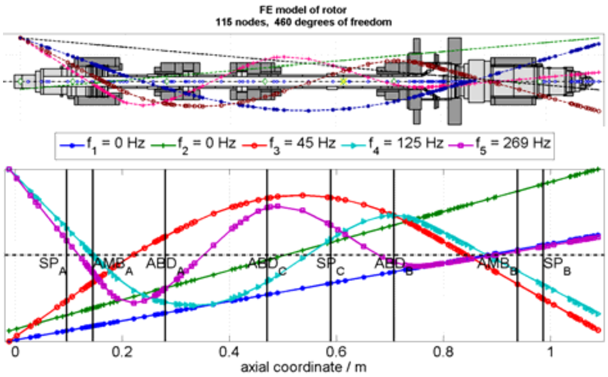

Fig. 4: FE-calculation results of the shaft without bearings

There are two rigid body modes and three bending modes in the frequency range up to 500 Hz. For the FE-calculation the influence of the clutch has been neglected. The FE-results have been fitted via modal analysis measurements. The first eigenfrequency at approx. 45 Hz illustrates the high dynamic flexibility of the shaft.

Fig 5 shows the block diagram of an AMB-rotor system in closed loop. It consists of magnetic actuators (power amplifiers and electromagnets), microprocessor (controller) and positions sensors [5]. AMBs use an actively controlled magnetic field to support the shaft without contact. A double-acting magnetic actuator geometry is used in two axes per bearing plane. Provided that the shaft oscillation is limited and closed to the centric position and that the amplifiers´ dynamic is negligible, the actuator behavior can be assumed to be linear. Thus the magnetic force acting in one direction is defined as:

$$F_{AML} = k_i\, i + k_s q \;\; with\; i = i_C + i_Z \qquad \text{(eq.2)}$$

with the linearised current gain $k_i = 214$ N/A and the negative position stiffness $k_s = 871$ N/mm. The additional actuating variable i_Z can be used for system identification or disturbance compensation.

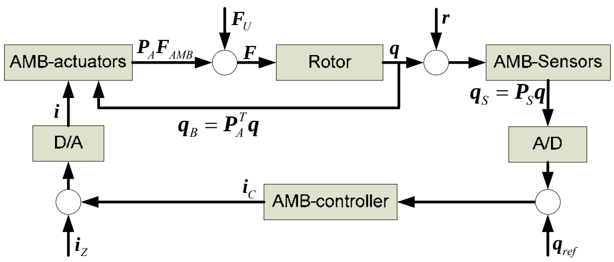

Fig. 5: AMB-rotor-system in closed loop

Because of the negative stiffness k_s, the AMB-rotor system is unstable [5]. For a stable operation of the AMB-rotor-system using a simple decentral controller, the collocation, the controllability and the observability properties of the shaft have to be accurately considered. At bearing A the 2nd bending mode is not controllable. Furthermore the 2nd and 3rd mode shapes at f_2 and f_3 have nodal point between the sensor and the AMB-actuator plane. Hence a phase lag of 180 ° exists and the control loop becomes unstable if this fact is not considered during the controller design. The situation in bearing B is not critical, because collocation is nearly achieved.

To stabilize the shaft a low gain proportional-derivative (PD) controller with the parameters $\boldsymbol{k}_P = diag(k_{p1},\dots,k_{pL})$ and $\boldsymbol{k}_D = diag(k_{D1},\dots,k_{DL})$ is used. Where $L = 4$ denotes the number of control values. Due to the small values of the controller parameters, the bearings are flexible. Hence the shaft oscillates during the operation on an orbit with a large diameter rising with present unbalance excitations $F_U = U\Omega^2$. The oscillations of the shaft in the magnetic bearings can be described with the following equation:

$$\boldsymbol{M}\ddot{\boldsymbol{q}} + \boldsymbol{B}_{AML}\dot{\boldsymbol{q}} + \boldsymbol{C}_{AML}\boldsymbol{q} = \boldsymbol{P}_A k_i \boldsymbol{i}_Z + \Omega^2[\boldsymbol{U}_0 + \boldsymbol{U}_{ABD}] \qquad \text{(eq.3)}$$

with

$$\begin{aligned} \boldsymbol{B}_{AML} &= \boldsymbol{D} + \Omega\boldsymbol{G} + \boldsymbol{P}_A k_i \boldsymbol{k}_D \boldsymbol{P}_S \\ \boldsymbol{C}_{AML} &= \boldsymbol{C} + \boldsymbol{P}_A[k_i \boldsymbol{k}_P \boldsymbol{P}_S - k_s \boldsymbol{P}_A^T] \end{aligned} \qquad \text{(eq.4)}$$

$\boldsymbol{P}_A$ and $\boldsymbol{P}_S$ describe the position of the actuators and the sensors along the shaft, $\boldsymbol{U}_0$ is the initial unbalance of the rotor and $\boldsymbol{U}_{ABD}$ the unbalance generated by the ABDs.

By suitable choice of the controller parameters $\boldsymbol{k}_P$ and $\boldsymbol{k}_D$ the stability and the dynamic of the shaft can be optimized. To know the influence of the magnetic bearings in closed loop as well as the critical speeds, which must be passed through to reach the operating speed, a second FE-calculation is performed. The FE-calculation results are depicted as in Fig. 6 as Campbell diagram of the shaft including the magnetic bearings in a frequency range between 0 Hz and 180 Hz.

The significant gyroscopic effect of the shaft yields forward and backward critical speeds, which are above and below their associated standstill natural frequencies (f_1 = 32 Hz, f_2 =74 Hz, f_3 = 88 Hz, f_4 = 125 Hz). The two lower bending modes (f_1 = 32 Hz, f_2 = 74 Hz) are the previously rigid body modes (f_1=0 Hz, f_2=0 Hz) of the free-free rotor (Fig. 4). In the case of unbalance only the forward critical speeds are excited. Other excitation, e.g. resulting of AMBs or non synchronous excitations can have a significant effect on the backward critical speeds.

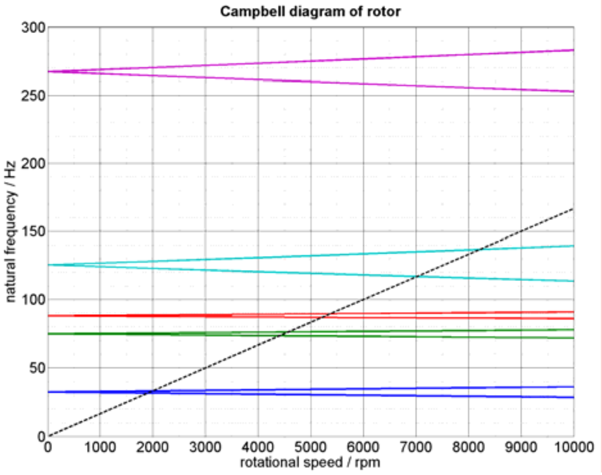

Fig. 6: Campbell diagram

Active balancing devices

An active balancing device is a typically mechatronic system which can contactless generate test and compensation weights during operation by means of a stepper motor drive principle and hence achieve an online variation of the unbalance state of a rotor. In this investigation the Hofmann – EMB 7000 Ringbalancer is used. Fig. 7 shows a scheme of the system. The shaft is equipped with three of these components. One Ringbalancer consists of a rotor part, which is mounted on the shaft as well as a stator part. Both parts are arranged in a centric position with a constant air gap of max. 1.5 mm.

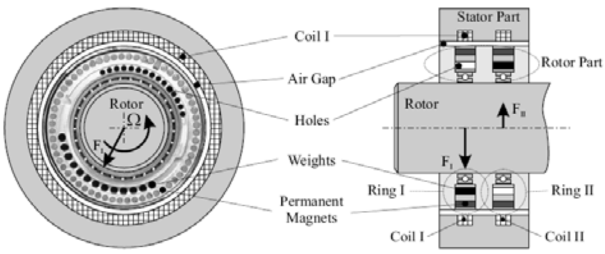

Fig. 7: ABD

ABD uses a mass-redistribution system consisting of two rings a and b, which are suspended on thin-section bearings, each with a certain unbalance capacity ($|U_a| = |U_b| = 100$ gmm). The rings are held in place relative to the rotor by permanent magnets and the axial distance between them is neglected, thus it can be viewed as one balancing plane. The magnitude $|U_{ABD}|$ and the position β_{ABD} of the generated unbalance in one plane is a result of the two rings´positions β_a and β_b:

$$|U_{ABD}| = |U_a|\sqrt{2 + 2\cos(\beta_a - \beta_b)} \\ \beta_{ABD} = [\beta_a + \beta_b]/2 \qquad \text{(eq.5)}$$

A maximum unbalance of 200 gmm can be generated by each ABD. The ABDs used in the test rig have two stepper motor type balance rings each with 60 detent increments per revolution. The worst case balance correction resolution for this configuration is $\pi/60 \approx$ 5,2 % of the maximum balance correction capacity of the device. Both rings can not be moved at the same time. An undesired effect of the Ringbalancer is a radial electromagnetic force, which excites the shaft during operation of the Ringbalancer [3].

Drive motor

The used high speed drive motor for the run up and run downs consists of an induction, synchronous motor controlled by a frequency converter. The motor from Lust Drive GmbH has a power of 11 kW, a nominal torque of 3.54 Nm, a nominal current of 23 A, is speed controlled and permits speeds up to 500 Hz.

AUTOMATIC BALANCING STRATEGY

The combination of AMBs, ABDs and DM allow for a fully automation of the balancing process with some further optimizations. While the AMBs are responsible for the stability of the AMB-rotor-system and measure the oscillations by their bearings sensors, the ABDs can control the vibration level under a tolerance value by changing the unbalance state of the rotor during operation. With the integrated DM, the rotating speed of the rotor during run ups and run downs can be controlled as function of the vibration level.

$$\Omega = \begin{cases} \dot{\Omega} t & if\ Q_m(t) < Q_{tol} \\ \Omega(t^*) & if\ Q_m(t^*) \geq Q_{tol} \end{cases} \qquad \text{(eq.6)}$$

$\dot{\Omega}$ denotes the acceleration, Q_m the vibration level at the sensor plane $m = 1 \ldots M$ and Q_{tol} the vibration limit. Consequently, the vibration level can be limited up to the operating speed. Thus the AMBs will stay linear and will not reach their saturation. Furthermore the AMB-rotor-system can be stabilised in a large frequency range with a simple decentral controller. The resisting torque due to the mass eccentricity will be negligible and a strong motor will not be necessary to accelerate when passing the critical speeds [6].

Fig. 8 shows the ***program for the automatic balancing strategy***. After initialisation and system check, the end user gives the setting parameter and starts the program. During the run up, the rotating speed and the oscillations of the shaft are uninterrupted measured. The ***balancing program*** (Fig. 9) is activated if vibration levels exceed a limit ($Q_m(t^*) \geq Q_{tol}$). After controlling vibration below the limit ($Q_m(t) < Q_{tol}$), the balancing program deactivates itself and permits the motor drive to continue its run up to the operating speed.

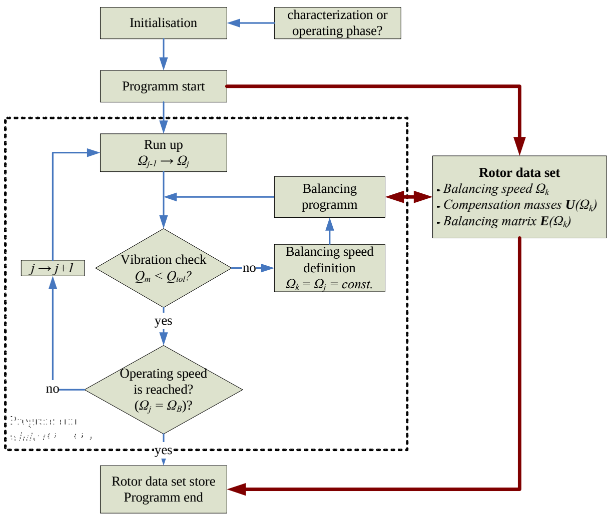

Fig. 8: Program for the automatic balancing strategy

The balancing program consists of two phases (Fig. 9), ***the characterization phase*** and ***the operating phase***. During the characterization phase the balancing speeds are determined and the influence coefficients as well as the compensation weights are estimated by means of test runs and stored in a rotor data set. In the operating phase the stored data of the rotor are used for a smooth run up or run down. With the known compensation weights from the characterization phase test runs are not anymore necessary during the operating phase. The ABDs have only to be moved to their compensation positions. Thus, this phase is faster than the other one. If the unbalance state changes during operation because of wear, thermic effects, variable load, or blade loss, the new compensation weight can be determined within seconds by means of a simple run without test weights.

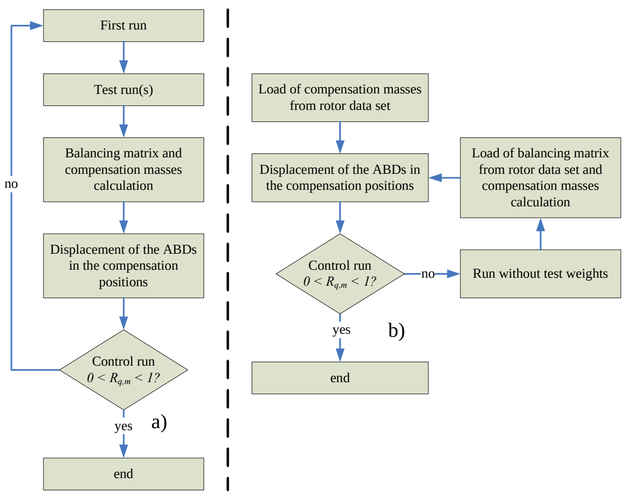

Fig. 9: balancing program: a) characterization phase, b) operating phase

For the realization of the automatic balancing strategy, following sub-functions are necessary.

1. A method to calculate the amplitude and the phase of the rotor synchronous vibrations at constant rotating speeds
2. A balancing method to determine the compensation weights
3. A strategy to define automatically the vibration limit depending on the residual vibrations after a balancing sequence.
4. A strategy to generate suitable test weights to avoid bad test runs and singular influence coefficients matrices.

Vibration measurement

The calculation of the amplitude and the phase of the rotor synchronous vibrations is performed by the Wattmeter method [6].

Balancing method

The most common methods for balancing are the influence coefficient method and the modal method [6]. The influence coefficient method is an experimental balancing procedure to reduce rotor synchronous vibrations to an allowable level using vibration data measured from sensor planes at a number of rotor speeds (balancing speeds), and the data of test weights added in different balancing planes. The calculated influence coefficients characterize the dynamic of the rotor. Because it is an entirely experimental procedure it is well suited for active balancing devices allowing automation without a priori knowledge. Furthermore, it is possible with the influence coefficient method to balance the rotor at any constant speeds not only in the vicinity of the critical speeds.

The influence coefficient method is based on the assumption of the rotor linearity between unbalances and oscillations:

$$\boldsymbol{q}_{0+ABD} = \boldsymbol{E}[\boldsymbol{U}_0 + \boldsymbol{U}_{ABD}] = \boldsymbol{q}_0 + \boldsymbol{q}_{ABD} \qquad \text{(eq.7)}$$

where $\boldsymbol{q}_{0+ABD}$ denotes a complex M row vector of measured vibrations at the M sensor planes, $\boldsymbol{E}$ a complex $M \times N$ matrix with influence coefficients of rotor, $\boldsymbol{U}_0$ a complex vector for the initial unbalance of rotor and $\boldsymbol{U}_{ABB}$ a complex N row vector for the N ABDs or balancing planes.

A total of $N+1$ runs at the same and constant rotating speed (balancing speed) $\Omega = r$ are necessary to calculate $\boldsymbol{E}$ and $\boldsymbol{U}_0$.

During the first run, the effects $q_{0+ABD,m}^r$ of the collective unbalance $\boldsymbol{U}_0^r + \boldsymbol{U}_{ABD}^{r-1}$ as well as the current generated unbalance vector $\boldsymbol{U}_{ABD}^{r-1} = \left[U_{ABD,1}^{r-1}, \dots, U_{ABD,N}^{r-1}\right]^T$ are measured respectively at each sensor plane $m = 1 \dots M$ and at each balancing plane $n = 1 \dots N$.

During the $n = 1 \dots N$ following test runs, test weights are simulated by moving the n^{th} ABD from the current position $U_{ABD,n}^{r-1}$ to a new one $U_{ABD,n}^r$ at the n^{th}

balancing plane. Furthermore, the effects $q^r_{n+ABD,m}$ of the collective unbalance $\boldsymbol{U}^r_0 + \boldsymbol{U}^{r-1}_{ABD} + [0, \dots, U^r_{T,n}, \dots, 0]^T$ as well as the current generated test weight $U^r_{T,n}$ are measured too. The generated test weight is given with the following equation:

$$U^r_{T,n} = U^r_{ABD,n} - U^{r-1}_{ABD,n} \qquad \text{(eq.8)}$$

Afterwards the balancing program calculates the influence coefficient matrix

$$\boldsymbol{E}^r = \begin{bmatrix} e^r_{1,1} & \cdots & e^r_{1,N} \\ \vdots & \ddots & \vdots \\ e^r_{M,1} & \cdots & e^r_{M,N} \end{bmatrix}, e^r_{m,n} = \frac{q^r_{n+ABD,m} - q^r_{0+ABD,m}}{U^r_{T,n}} \qquad \text{(eq.9)}$$

The compensation unbalance vector $\boldsymbol{U}^r_{ABD,ref}$ is finally determined through transformation of eq. 7:

$$\boldsymbol{U}^r_{ABD,ref} = \boldsymbol{U}^{r-1}_{ABD} - [\boldsymbol{E}^r]^{-1}\boldsymbol{q}^r_{0+ABD} \qquad \text{(eq.10)}$$

After displacement of the ABDs in the compensation positions $\boldsymbol{U}^r_{ABD} \approx \boldsymbol{U}^r_{ABD,ref}$, a control run is done:

$$\boldsymbol{q}^r_{after} = \boldsymbol{E}[\boldsymbol{U}^r_0 + \boldsymbol{U}^r_{ABD}] \qquad \text{(eq.11)}$$

followed by the determination of the balancing performance $R^r_{q,m}$, of the unbalance reduction ratio $R^r_{U,n}$, and of the balancing success S^r:

$$\begin{aligned} R^r_{q,m} &= 1 - |q^r_{after,m}|/|q^r_{0+ABD,m}| \\ R^r_{U,n} &= |U^r_{ABD,n}|/|U^r_{ABD,ref,n}| \\ S^r &= \begin{cases} 1 \; if \; Q_m = |q^r_{after,m}| < Q_{tol} \\ 0 \; if \; Q_m = |q^r_{after,m}| > Q_{tol} \end{cases} \end{aligned} \qquad \text{(eq.12)}$$

If $0 < R^r_{q,m} < 1$, then the balancing program deactivates itself, else wise new iterations are started until the break condition is reached. But the number of iterations is limited, because the situation can occur, where the vibrations can not be reduced e.g. if the ABDs are saturated.

Strategy to generate suitable test weights

The goal of the generation of test weights is the calculation of the influence coefficients by experimental tests. Bad test runs with $|q^r_{n+ABD,m}| = 0$ or $|q^r_{n+ABD,m}| \approx |q^r_{0+ABD,m}|$ lead to a singular influence coefficient matrix and increase the expenditure of the time. To avoid this problem, suitable test weights have to be generated. A strategy for this purpose looks like follows: the trial masses (eq. 8) are generated until eq. 13 is fulfilled at all sensor planes.

$$\left||q^r_{n+ABD,m}| - |q^r_{0+ABD,m}|\right|/|q^r_{0+ABD,m}| \geq \Delta q \qquad \text{(eq.13)}$$

In that way a certain deviation between $|q^r_{n+ABD,m}|$ and $|q^r_{0+ABD,m}|$ is reached.

Strategy to define the allowable vibration level

Vibration limits are typically selected as criteria for determination of balancing speeds and thus for enabling and disabling active balancing control [2]. To eleminate the need to apply special engineering knowledge in setting these limits for each application, an automatic online limit selection algorithm is also necessary.

One should set activation limits as low as possible to ensure that low vibration levels are achieved. However measurement errors $|\boldsymbol{q}_{errors}|$, resolution and capacity limitations (residual unbalance, $|\boldsymbol{q}_{unbalance}|$) of the ABD constrain just how low the vibration oscillation $|\boldsymbol{q}^r_{after}|$ can be controlled. The allowable vibration level is defined as:

$$Q_{tol} \geq |\boldsymbol{q}^r_{after,max}| \approx |\boldsymbol{q}_{errors}| + |\boldsymbol{q}_{unbalance}| \qquad \text{(eq.14)}$$

where $|\boldsymbol{q}^r_{after,max}|$ denotes the maximal vibration level at the sensor planes. However, because of the non existent residual unbalance at the beginning of the balancing process, the following equation is used:

$$Q^{r=1}_{tol} = Q_{tol,init} \geq \alpha|\boldsymbol{q}_{errors}| \; with \; \alpha > 1 \qquad \text{(eq.15)}$$

where $|\boldsymbol{q}_{errors}|$ is given with the sensitivity of the measurement system. During operation and after some balancing sequences the residual unbalance, which depends on the resolution and on the capacity of the ABDs, can be arbitrary very large. A strategy to define the allowable vibration level during operation looks like follows:

$$Q^{r+1}_{tol} = \begin{cases} \alpha|\boldsymbol{q}^r_{after,max}|, & case\ 1 \\ Q_{tol,init}, & case\ 2 \end{cases} \qquad \text{(eq.16)}$$

Case 1 is valid, if the tolerance value is smaller than the residual vibrations and if the ABDs are saturated $\left(Q^r_{tol} < |\boldsymbol{q}^r_{after,max}| \text{ and } |U^r_{ABD}| > |U_{ABD,max}|\right)$. Case 2 is valid if case 1 is not fullfilled $\left(Q^r_{tol} > |\boldsymbol{q}^r_{after,max}|\right)$.

Special case: If the tolerance value after several balancing sequences is still higher than the residual vibrations by not saturated ABDs $\left(Q^r_{tol} < |\boldsymbol{q}^r_{after,max}| \text{ and } |U^r_{ABD}| < |U_{ABD,max}|\right)$, then one ABD is probably close to a nodal point and has no influence on the unbalance state. In this case this frequency range has to be skipped.

Furthermore, unbalance compensation at critical speeds should be avoided. Because of its high sensitivity, the system can be destabilized during test runs. Therefore the shaft has to be always balanced ahead the critical speed, before passing the critical speed.

EXPERIMENTAL RESULTS

To validate the efficiency of the proposed automatic balancing strategy, experiments on the test rig are performed. Because of the low capacity of the ABDs (200 gmm) and large vibrations in the rotor center, it is suitable to reduce the vibrations only at the bearing planes so that the ABD in the center of the rotor is not used.

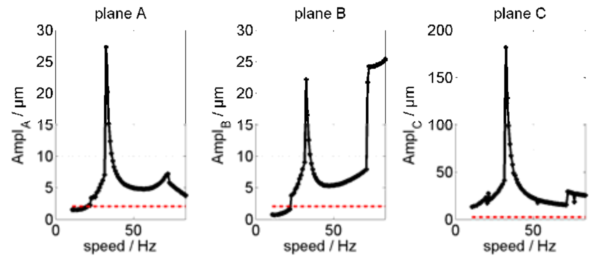

Fig. 10: run up without automatic balancing strategy

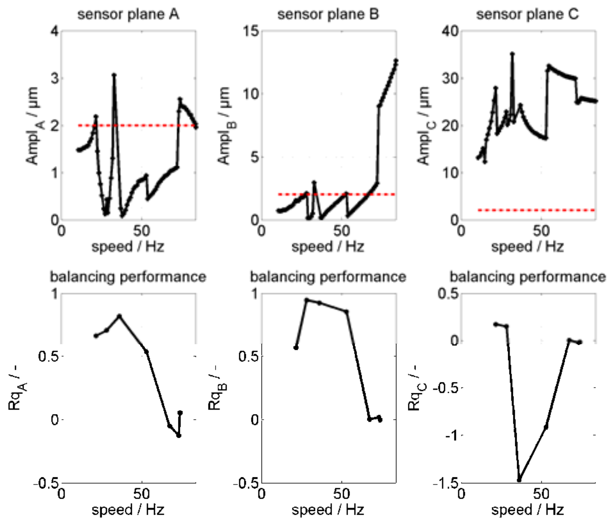

Fig. 11: run up with automatic balancing strategy and balancing performance at the balancing speeds

Fig. 10 shows a run up without automatic balancing strategy up to 80 Hz. By passing the first critical speed at 32 Hz, oscillations with large amplitude occur. They reach at bearing A 30 µm, at bearing B 25 µm and in the center of the rotor at the sensor plane C 200 µm.

By the same run up with the automatic balancing strategy, with $Q_{tol,init} = 2$ µm, $\Delta q = 5\%$ and $\alpha = 1.5$ (Fig. 11), the maximal vibration levels reached 3 µm at bearing A, 3 µm at bearing B and 35 µm at the sensor plane C by passing the 1st critical speed. Because of saturated ABDs (Fig. 12) it is not possible to reduce the vibration levels after passing the 2nd critical speed at approx. 73 Hz. Therefore the vibrations become larger and reach e.g. 12 µm at 80 Hz at bearing B.

Fig 12 shows the estimated unbalance magnitude and the unbalance reduction ratio (R_u) at the balancing speeds. Up to 60 Hz, the vibration limit of 2 µm is not violated, the ABDs are not saturated, the unbalance reduction ration is close to one and the balancing performance is far away from zero. Over 60 Hz in the vicinity of the 2nd critical speed, the ABDs are saturated. Thus the vibrations can not be anymore reduced and the allowable vibration level has to be adapted (eq. 16). Furthermore in this frequency range the balancing performance is close to zero and the unbalance reduction ratio is far away from zero. The conclusion can be done, that the strategy works very well as long as the ABDs are not saturated or are not on a nodal point.

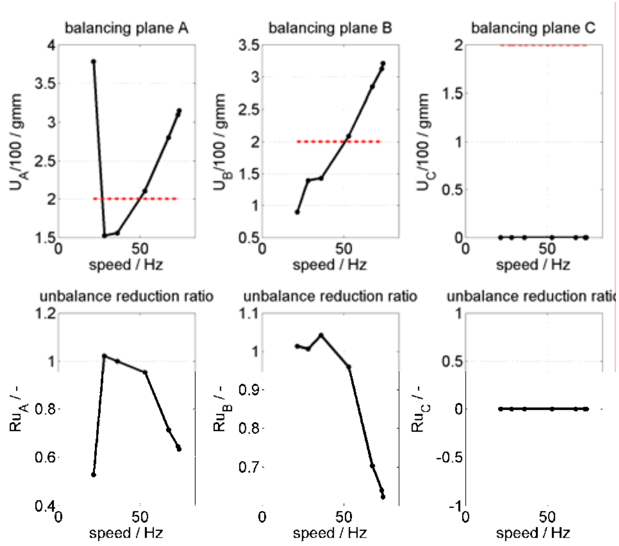

Fig. 12: estimated unbalance magnitude and unbalance reduction ratio at the balancing speeds

CONCLUSION

This paper presents a strategy for automatic balancing of flexible rotors based on the combination of three kinds of active systems: active magnetic bearings, active balancing devices and drive motor. The automatic balancing strategy allows complete automation of the balancing process and limits vibration levels up to the operating speed. Hence it assures the precision, the reliability, and the operational safety of high speed machinery. Experiments on a test rig show the efficiency and the feasibility of the strategy.

In next investigations, the capacity of the ABDs are going to be increase, in that way more critical speeds can be passed without deterioration of the unbalance state.

References

[1] S. Zhou and J, Shi. "Active balancing and vibration control of rotating machinery: A survey", The Shock and Vibration Digest, vol. 33, no. 4, pp. 361-371, July 2001.

[2] S. W. Dyer, J. Ni, Z. Zhuang and J. Shi, "Auto-tuning adaptive supervisory control of single plane active balancing systems", Vibration Control, NAMRC XXVII, May 24-26, 2000, University of Kentucky, Lexington, Kentucky.

[3] K. Adler, D. Neumeuer and R. Nordmann, „Active Unbalance generation for failure simulation in turbo engines“, ACTIVE04 the 2004 International Symposium on Active Control of Sound and Vibration, September 2004.

[4] K. Adler, B. Aeschlimann and R. Nordmann, „Active Balancing of a Supercritical Rotor on Active Magnetic Bearings“, ISMB10 the 10th International Symposium on Magnetic Bearings, August 2006, Martigny, Switzerland.

[5] T. Krüger, M. Aenis, D. Neumeuer, U. Schönhoff and R. Nordmann, „Modellbildung und Reglerentwurf zu aktiven Magnetlagersystemen für elastischen Rotoren", Schwingungen in rotierenden Maschinen V, Frebruary 2001.

[6] A. Lingener, „Auswuchten – Theorie und Praxis", Verlag Technik Berlin – München, 1992.

[7] D. Neumeuer, M. Kaufeld, „Active Balancing for high speed machining – objectives and limits", Seventh International Conference on HIGH SPEED MACHINING 2008.